Calculation of Frequency-Dependent Parameters of Power Cable Arrangements Using Pixel-Shaped Conductor Subdivisions

R. A. Rivas (*) J. R. Martí

Department of Electrical and Computer Engineering, The University of British Columbia
2356 Main Mall, Vancouver, BC, Canada, V6T 1Z4.
(*) on a leave of absence from Universidad Simón Bolívar, Departamento de Conversión y Transporte de Energía,
Valle de Sartenejas, Baruta, Caracas, Edo. Miranda, Venezuela, Apartado Postal 89000.

Abstract - **A methodology for frequency-dependent parameter calculations of arbitrarily-shaped power cable arrangements is presented. This method is based on subdividing the cable geometry into pixel-shaped (square-shaped) partial subconductors, considering a homogeneous automatic spatial discretization of its cross section. Subsequently, traditional partial subconductor-based methods are used to reduce the impedance matrix, and to obtain the series cable parameters (resistance and inductance). A simple cylindrical coaxial case is studied, and the results are compared with those given by cable parameter routines based on Bessel function solutions.**

Keywords: Frequency-Dependent Cable Parameters, EMTP

I. Introduction

Frequency-dependent power cable models are needed for accurate simulation of fast transients in electric power systems. However, given the wide variety of complex geometric shapes, materials used, arbitrary configurations, as well as the presence of strong skin and proximity effects among conductors, power cable parameter calculations can be a difficult task.

Two main approaches have been suggested in the past for frequency-dependent cable parameter calculations: analytical solutions [1] and numerical ones. The numerical methods have also been divided into approximations based on: finite elements [2] and partial subconductors [3, 4]. Techniques based on analytical solutions have been used in the past to solve simple geometries such as those made up of concentric cylindrical conductors. Techniques based on numerical procedures, on the other hand, have been suggested to study cables with eccentric conductors as well as arbitrary shapes and configurations.

The Finite Element approach solves the problem of calculating power cable parameters of arbitrary shapes and geometries elegantly. This technique, nevertheless, presents two disadvantages. On the one hand, the generation of the finite element mesh requires much user expertise, and intervention, since it must be suitable for both geometry and physics of the particular situation. On the other hand, the open-boundary (semi-infinite) nature of the earth-return path increases the amount of necessary calculations.

Partial subconductor-based methods avoid the above-mentioned open-boundary problems by considering asymptotic expressions for the earth-return path [5]. However, they still require considerable user intervention to set up the subconductor coordinates and define the most appropriate shapes and number of subconductors given an arbitrary configuration.

A new partial subconductor method for frequency-dependent parameter calculations of arbitrarily-shaped power cable arrangements is presented. The method is based on subdividing the cable geometry into pixel-shaped (square-shaped) partial subconductors, considering an automatic spatial discretization of its cross section.

The main idea is to start with a digital image (pixel map) of the cross section of the cable arrangement and automatically identify the spatial coordinates of pixel-shaped partial subconductors that make up the different conductive layers. Image resolution and penetration depth techniques are then used to optimize the number of subconductors and to set up the boundaries among the different conductive parts.

A simple cylindrical coaxial case is studied with the proposed technique, and the results are compared with those given by common cable parameter routines based on Bessel function solutions.

II. Analysis of the Modeling Problem

The problem under study is typical of power system component parameter calculations: given the component geometry and the electric properties of the material (conductivity, permeability, and permittivity), the corresponding electric parameters have to be determined. Since the idea starts with the use of an image, these steps have to be followed: the image has to be acquired, digitized, and subjected to modules of preprocessing, segmentation, representation, description, recognition, and interpretation, under the supervision of a knowledge base [6].

The problem domain in this case is made up of cross section drawings of power cable arrangements. The objective is to determine the frequency-dependent series parameters (resistance and inductance) suitable for electromagnetic transient studies. The image, thus, has to be acquired and discretized at both spatial coordinates and discrete color values to distinguish among conductor and insulation regions.

To acquire and digitize the image two options can be considered. On the one hand, the cable layout can be traced with technical drawing computer programs capable of discretizing and saving the image in conventional digital image formats. On the other hand, a scale drawing can also be scanned and saved using the same aforementioned formats. Regardless of the option, the file stores equally spaced samples of a rectangular matrix in which each element is a discrete color (or gray-level) value.

The segmentation step extracts individual conductors from the background and yields the raw partial subconductor data in which space coordinates and discrete colors of both conductive regions and insulation are stored. It is

assumed that all distinct conductive regions (cores, sheaths, armors, etc.) are assigned different colors intensity values. A regional representation of the segmentation process, instead of a boundary one, is therefore considered appropriate.

The representation step transforms the raw data into a form appropriate for computer analysis, and the description step converts these data into the quantitative information of interest. Since the image has to be analyzed precisely from a mathematical point of view, conventional non-lossy digital image formats such as bitmap (uncompressed) and GIF (Graphical Interchange Format, which is compressed) can be used to represent it. Taking into account that current desktop computers commonly have gigabytes of storage facilities in their hard disks, large files represent no problem.

The aforementioned formats also enable the easy retrieval of the variables of interest which describe the image with quantitative values. As a result, a simple bidimensional array is sufficient. Rows and columns yield the spatial coordinates of the subconductors (pixels), whereas the matrix elements give the colors. It is unlikely that practical power cables have more than, perhaps, 50 distinct conductive regions; 256 colors are therefore more than enough to describe all possible situations.

According to the above points, one byte is more than sufficient to store the color of each subconductor. Next, spatial coordinates are converted into actual dimensions since both resolution (pixels per unit length) and scale factor (drawing length/actual length) are known.

The recognition step deals with the process of labeling the different regions. It is necessary to identify conductors (cores, sheaths, armors, etc.), screens, insulation, and ground. Once the algorithm recognizes the number of connected components (number of regions with different colors), the process of identifying which color corresponds to what conductor, insulation, and/or ground relies on the user.

The interpretation step assigns a meaning to the different conductive regions. For instance, the dc resistance per subconductor and Geometric Mean Distances (GMD's) among them are calculated in this phase. Also, penetration depths are compared with subconductor dimensions, in order to determine if the resolution used is fine enough to accurately represent skin effects; otherwise, the resolution is increased automatically by subsampling pixels.

Normally, a drawing is used to define the cable geometry, but a photograph can be used as well. In that last case, it is necessary to acquire and digitize the image by scanning the cross-section picture and preprocessing it in order to remove noise, extract conductive and insulating regions from the background, and, perhaps, to smooth edges and change colors.

III. Proposed Methodology

Let us suppose that the continuos image of a power cable cross section, illustrated in Fig. 1, is discretized in both spatial coordinates and colors. Let us also assume that the samples are equally spaced, and that the colors of the partial subconductors or pixels are denoted by integer quantities. The discrete image is then represented by a two dimensional matrix with integer number elements which can be retrieved from a non-lossy graphic format input file. The lower the resolution or degree of discernible detail, the more the so-called checkerboard effect becomes visible, and the worse the approximation becomes as depicted in Fig. 2.

Each conductor is represented by a different color or gray-level. Insulation is denoted by another distinct color as well (e.g.: white). Therefore, each one of the connected components or regions is identified by subconductors of the same color. These results are summarized through a histogram in which the number of occurrences per color is specified. Fig. 3 illustrates, for simplicity, the case of lowest resolution. The coordinate axes are defined following the traditional conventions of Digital Image Processing: rows represent x-coordinates (vertical position) and columns y-coordinates (horizontal position).

Let us make the following assumptions as well [2, 7]:

1) The conductors are rectilinear, parallel to each other, and longitudinally homogeneous, so spiraling effects are not taken into account. They are also considered long enough to make the problem two-dimensional.

2) The space, all conductors, and insulation have homogeneous permeability. The permeability is also constant, so non-linear effects are neglected.

3) Displacement currents are ignored.

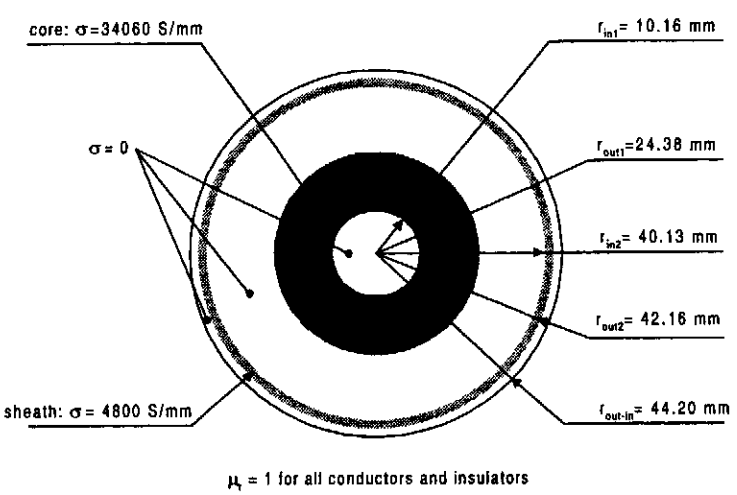

Fig. 1: Cross section of a coaxial single-core cable

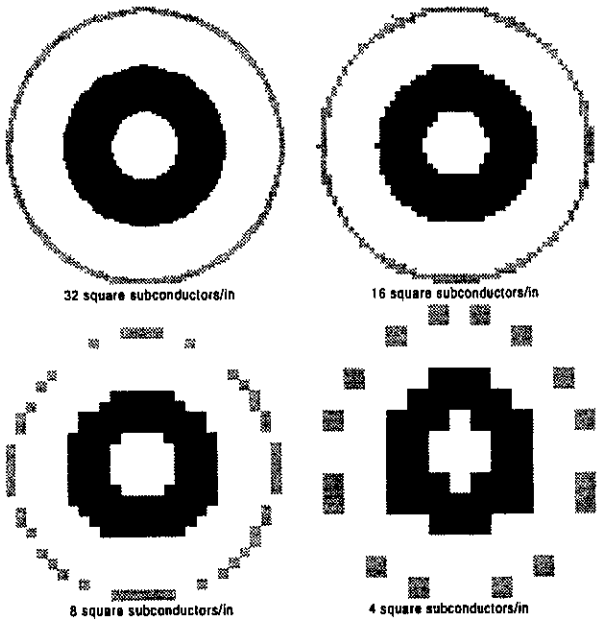

Fig. 2: Effect of changing the spatial resolution

4) TEM propagation is assumed in calculating the series impedances.

The steps of the developed algorithm are then indicated as follows:

Step 1 (acquisition and discretization): draw or scan the cable arrangement layout.

Step 2 (representation): save this scale model in a non-lossy graphic format file.

Step 3 (reading input data): read the aforementioned input file in which image sampling and color (or gray-level) quantization are stored; read also resolution, scale factor, conductor resistivities, and frequencies for which parameters are desired.

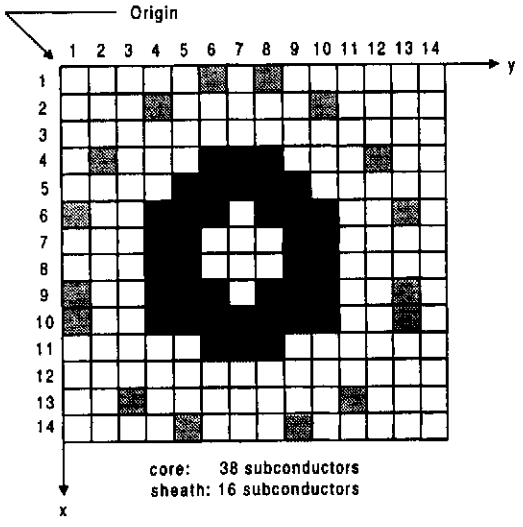

Fig. 3: Coordinate system for homogeneous space discretization (4 subcond./in)

Step 4 (recognition): determine the number of different regions (number of conductors and insulation) by looking for distinct colors (or gray-levels); determine also the number of occurrences (subconductors) per region; name the different regions as $core_1$, $sheath_1$, $insulation_1$, etc. by asking the user to identify each one.

Step 5 (segmentation): extract conductors from insulation and background by looking for colors previously assigned to conductive regions; store coordinates of every partial subconductor forming part of a conductive region.

Step 6 (description): shift all x-and y-coordinates half a partial subconductor (pixel) and transform them into actual values by dividing by both scale factor and resolution.

Step 7 (interpretation): calculate DC resistances and self geometric mean distances per partial subconductor as in [3, 8]:

$$r_i = \frac{1}{\sigma_i A_i} \tag{1}$$

$$gmd_i = 0.44705 a_i \tag{2}$$

in which:
r_i: dc resistance of partial subconductor i in Ω/km
gmd_i: self geometric mean distance of partial subconductor i in meters
σ_i: conductivity of partial subconductor i in S/km
A_i: area of partial subconductor i in square kilometers
a_i: side of partial subconductor i in meters

Step 8 (interpretation): calculate mutual geometric mean distances among partial subconductors as in [8, 9]:

for partial subconductors lying along the same y-coordinate:

$$gmd_{ij} = |x_i - x_j| \tag{3}$$

for partial subconductors lying along the same x-coordinate:

$$gmd_{ij} = |y_i - y_j| \tag{4}$$

for partial subconductors not lying along the same y-or x-coordinate:

$$\ln(gmd_{ij}) = -\frac{1}{a_i^4}\{\frac{(x-x')^4-6(x-x')^2(y-y')^2+(y-y')^4}{24} * \sqrt{\ln[(x-x')^2+(y-y')^2]} - \frac{(x-x')(y-y')}{6}[(x-x')^2\tan^{-1}(\frac{y-y'}{x-x'})+ +(y-y')^2\tan^{-1}(\frac{x-x'}{y-y'})]\}\Big|_{x_1}^{x_2}\Big|_{x_1'}^{x_2'}\Big|_{y_1}^{y_2}\Big|_{y_1'}^{y_2'} - \frac{25}{12} \tag{5}$$

in which:
gmd_{ij}: mutual geometric mean distance between partial subconductor i and partial subconductor j in meters
x_i: central x-coordinate of partial subconductor i in meters
y_i: central y-coord. of partial subcond. i in meters
x_1: upper side x-coord. of partial subcond. i in meters
x_2: lower side x-coord. of partial subcond. i in meters
y_1: left-hand side y-coord. of partial subcond. i in meters
y_2: right-hand side y-coord. of partial subcond. i in meters
x_1': upper side x-coord. of partial subcond. j in meters
x_2': lower side x-coord. of partial subcond. j in meters
y_1': left-hand side y-coord. of partial subcond. j in meters
y_2': right-hand side y-coord. of partial subcond. j in meters

Step 9 (interpretation): calculate self and mutual inductances among loops of partial subconductors, considering

a circular-shaped fictitious return path (assumed as a perfect conductor) closing in on the cable arrangement cross section, as follows:

$$L_{ii} = \frac{\mu}{2\pi} 10^3 \ln\left(\frac{r_{ring}}{gmd_i}\right) \quad (6)$$

$$L_{ij} = \frac{\mu}{2\pi} 10^3 \ln\left(\frac{r_{ring}}{gmd_{ij}}\right) \quad (7)$$

in which:

L_{ii}: self inductance of loop made up of partial subconductor i and circular-shaped return path closing in on the cable arrangement in H/km

L_{ij}: mutual inductance between loop made up of partial subconductor i and aforementioned circular-shaped return path and the loop of partial subconductor j and the same circular-shaped return path in H/km

μ: constant of permeability in H/m

r_{ring}: radius of aforementioned circular-shaped and infinitely thin return path in meters

gmd_i, gmd_j: geometric mean distances as defined at steps 7 and 8

Step 10 (knowledge base) [4, 7]: sort self and mutual inductances in a two dimensional array as follows: rows of first conductor's partial subconductors (e.g. core) from position *1* to $ntsc_1$, rows of second conductor's partial subconductors (e.g. sheath) from position $(ntsc_1 + 1)$ to $(ntsc_1 + ntsc_2)$, and so forth from top to bottom. Apply also the above order to columns from left to right.

$ntsc_1$: is the 1st conductor's total number of partial subconductors

$ntsc_2$: is the 2nd conductor's total number of partial subconductors

Step 11 (knowledge base): construct matrix of complex impedances at frequency f_k following the order indicated in step 10, and as shown below:

$$Z_{ii} = r_i + j\omega_k L_{ii} \quad (8)$$

$$Z_{ij} = j\omega_k L_{ij} \quad (9)$$

in which:

f_k: k[th] frequency for which parameters are desired in Hz

ω_k: k[th] angular frequency ($2\pi f_k$) in rad/sec

j: imaginary number equal to $(-1)^{1/2}$

Z_{ii}: complex self impedance of loop made up of partial subconductor i and circular-shaped return path in Ω/km

Z_{ij}: complex mutual impedance between loop made up of partial subconductor i and circular-shaped return path and the loop of partial subconductor j and circular-shaped return path in Ω/km.

Step 12 (knowledge base): sort, modify, triangularize, and reduce the matrix of complex impedances at frequency f_k, and impose the zero current condition on the fictitious return path as in [4, 7]. Compute resistances $r_{ij}=Re\{Z_{ij}\}$ and inductances $L_{ij}=Im\{Z_{ij}\}/\omega_k$.

Step 13: go back to Step 11 if more frequencies are left over; else stop.

IV. Results

The series resistance and inductance corresponding to the geometry depicted in Fig. 1 were calculated using the proposed methodology. Table I indicates the number of resultant subconductors as a function of resolution after applying homogeneous automatic spatial discretization to the entire cross section and after transforming the continuos image into a digital image with bitmap format.

Figs. 4 and 5 show the frequency-dependent parameters (resistance and inductance) obtained as a function of spatial resolution, considering frequencies and spatial resolutions up to 100 kHz and 20 subconductors/inch, respectively. The results are also compared with those given by analytical techniques based on Bessel function solutions.

Table I shows that the necessary number of subconductors and, therefore, the requirements of computer memory, grow noticeably as the resolution is increased. For a much finer subdivision of 20 subconductors/inch, 1274 subconductors are generated, whereas for a resolution of 4 subconductors/inch, 54 subconductors barely show up.

Figs. 4 and 5, respectively, indicate that the model works correctly; the typical behavior for skin and proximity effects is observed in the frequency-dependent resistances and inductances. Whereas resistance increases as

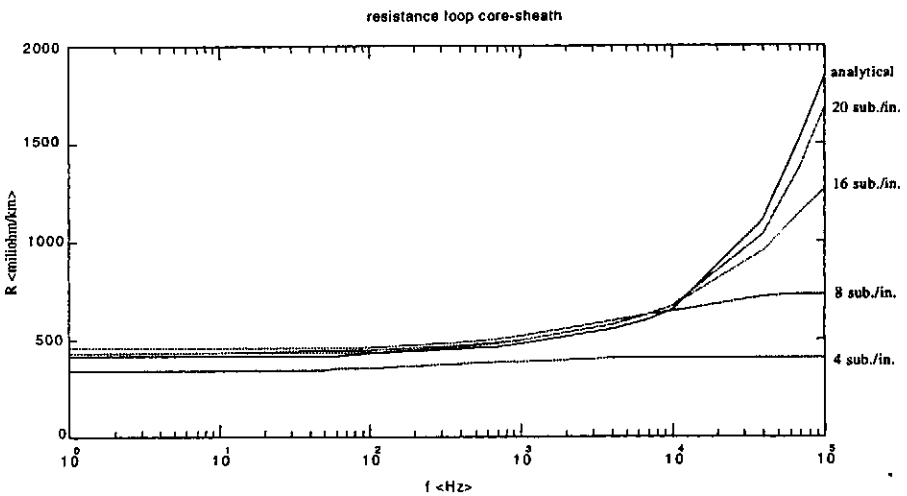

Fig. 4: Resistance as a function of frequency for different spatial resolutions

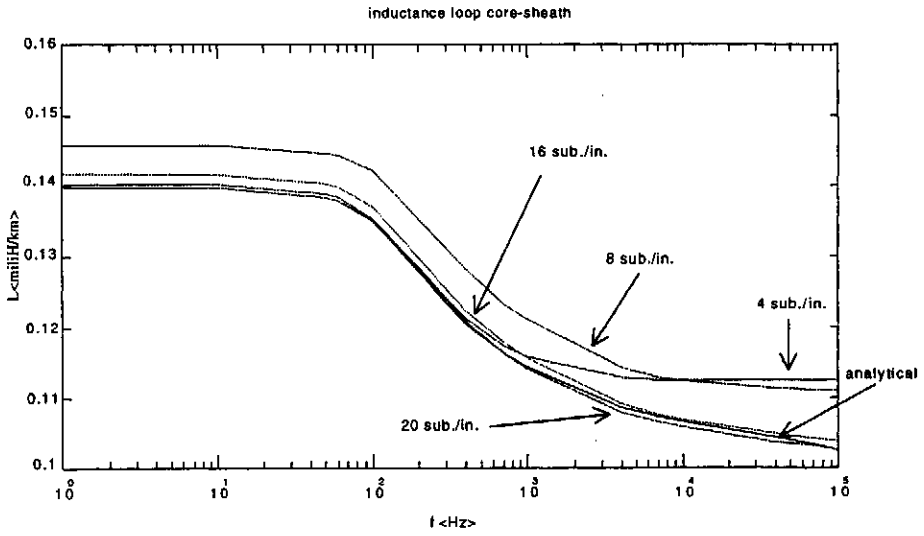

Fig. 5: Inductance as a function of frequency for different spatial resolutions

the frequency grows, inductance decreases since less magnetic flux linkages are inside the conductors. The loop inductance [7], therefore, tends to a constant value given by zero internal inductances $L_{core\text{-}out}$ and $L_{sheath\text{-}in}$, and the nonfrequency-dependent inductance $L_{core\text{-}sheath/insulation}$ which, in this case, represents the inductance due to the external magnetic flux. The loop resistance increases with frequency since currents tend to flow through the outermost and innermost layers of core and sheath, respectively. As a result, less cross-sectional area is available for currents to flow through.

As expected, errors are lower as spatial resolutions are increased. Errors of resistances are lower than 4.79 % below frequencies of 10 kHz when using resolutions of 16 and 20 subconductors/inch. Errors of inductances are lower than 1.43 % and 0.82% at all frequencies when using resolutions of 16 and 20 subconductors/inch, respectively.

As can be observed in Fig. 4, errors of resistances above frequencies of 40 kHz are always lower as spatial resolutions are increased. For a resolution of 20 subconductors/inch, which yields the best results, errors are lower than 9.65 %. A cut-off resistance shows up as well at frequencies for which resolutions are not fine enough to take skin effects into consideration. To avoid such a problem, subdivisions must be finer than the penetration depth δ [9].

Resolution calculations are based on using the lowest δ, in this case the core's, which has the highest conductivity, and considering that, given the existing circular symmetry, the hypotenuse of every square subconductor must be, at least, equal to δ. Therefore, the minimum resolution per frequency required to avoid the cut-off effect is obtained applying (10). When δ is greater than the smallest thickness, the thickness is taken to determine the appropriate resolution:

$$res_k = \frac{\sqrt{2}}{\delta_k} \tag{10}$$

in which:

$$\delta_k = \frac{1}{\sqrt{\pi \mu \sigma f_k}} \tag{11}$$

and res_k is equal to resolution in subconductors per meter at frequency f_k and δ_k is equal to penetration depth in meters at frequency f_k.

V. Conclusions

A methodology to calculate frequency-dependent parameters of arbitrarily-shaped power cable arrangements based on the automatic spatial discretization of its cross section and partial subconductor techniques has been presented.

Standard graphic formats are used to set up subconductor coordinates of cable configurations, given either their manufacturer drawings or their pictures of actual cross-sections. The use of such graphic format files is a novel approach which overcomes the difficulties associated with arbitrarily-shaped power cables.

Given the widespread use and acceptance of these graphic formats, the new solution technique promises to provide a flexible cable parameter calculation tool for EMTP-type studies.

VI. Acknowledgement

The financial assistance of "El Consejo Venezolano de Investigaciones Científicas y Tecnológicas (CONICIT)" and "La Universidad Simón Bolívar", Caracas, Venezuela, in this research project is gratefully acknowledged. The authors would also like to thank Dr. H. W. Dommel of The University of British Columbia for his helpful discussions and suggestions.

Table I: Number of subconductors as a function of resolution

Resolution	number of subcond.	
<subcond/in>	core	sheath
4	38	16
8	134	48
16	598	202
20	963	311

VII. References

[1] A. Ametani, "A General Formulation of Impedance and Admittance of Cables", *IEEE Trans. on Power App. Syst.*, Vol. PAS-99, No 3, May/June 1980, pp.902-910.

[2] Y. Yin, H. W. Dommel, "Calculation of Frequency-Dependent Impedances of Underground Power Cables with Finite Element Method", *IEEE Trans. on Magnetics*, Vol. MAG-25, July 1989, pp. 3025-3027.

[3] P. Graneau, *Underground Power Transmission*, John Wiley & Sons, New York, 1979.

[4] P. de Arizón, H. W. Dommel, "Computation of Cable Impedances Based on Subdivision of Conductors", *IEEE Trans. on Power Delivery*, Vol. PWRD-2, January 1987, pp. 21-27.

[5] L. M. Wedepohl, D. J. Wilcox, "Transient Analysis of Underground Power-Transmission Systems; System-Model and Wave-Propagation Characteristics", *Proc. IEE*, Vol. 120, February 1973, pp. 252-259.

[6] González R., Woods R., *Digital Image Processing*, Addison-Wesley Publishing Company Inc., 1992.

[7] H. W. Dommel, *EMTP Theory Book*, Microtran Power System Analysis Corporation, Vancouver, B.C., Canada, May 1992, last update April 1996.

[8] P. Oeding, K. Feser, "Geometric Mean Distances of Rectangular Conductors" (in German), *ETZ-A*, Vol. 86, No 16, 1965, pp. 525-533.

[9] W. T. Weeks, L. L. Wu, M. F., McAllister, A. Singh, "Resistive and Inductive Skin Effect in Rectangular Conductors", *IBM Journal of Research and Development*, Vol. 23, No 6, pp. 652-660, November 1979.